The impact of aggregation on the biodistribution of hypericin

MARIE VAN DE PUTTE[1], TANIA ROSKAMS[2], GUY BORMANS[3], ALFONS VERBRUGGEN[3] and PETER A.M. DE WITTE[1]

[1]Laboratorium voor Farmaceutische Biologie en Fytofarmacologie, Faculteit Farmaceutische Wetenschappen; [2]Afdeling Histochemie en Cytochemie, Faculteit Geneeskunde; [3]Laboratorium voor Radiofarmaceutische Chemie, Faculteit Farmaceutische Wetenschappen, K.U. Leuven, Belgium

Received September 5, 2005; Accepted October 21, 2005

Abstract. Hypericin is a potent agent in the photodynamic therapy of cancers and accumulates to a large extent in tumor tissue. To better understand the impact of hypericin aggregates present in the delivery vehicle on the biodistribution of the compound, we compared the *in vivo* tissue accumulation after administering hypericin suspended as coarse aggregates in phosphate-buffered saline, with the biodistribution found after injection of a solution of hypericin in a mixture of DMSO, polyethylene glycol and water. When administered as coarse aggregates, hypericin showed a pronounced uptake in liver, spleen and lung and a slow body clearance with a complete decline in tumor/normal tissue ratios (far less than 1). In contrast, delivery of hypericin as a solution resulted in dramatically improved tumor to normal tissue ratios and a relatively fast elimination from the body. To elucidate the exact localization of hypericin in both conditions, a fluorescence microscopy study was performed on sections of spleen, liver, lung and tumor tissue. At 24 h after injection, fluorescence in spleen, liver and lung was faint and homogeneous for dissolved hypericin, whereas bright fluorescent spots covering the entire tissue sections were found when coarse aggregates were injected. We found that aggregates get trapped within these tissues, followed by a gradual monomerization. A direct involvement of monocytes and macrophages, however, could not be demonstrated. In conclusion, it is of critical importance that the delivery vehicle prevents extensive aggregation of hypericin before injection and assures an efficient transfer to serum lipoproteins upon injection. These results may also be extended to radiolabeled derivatives and other lipophilic photosensitizers, such as porphyrins, phthalocyanines, naphthalocyanines and chlorines, with similar aggregation properties.

Correspondence to: Dr Peter A.M. De Witte, Laboratorium voor Farmaceutische Biologie, Faculteit Farmaceutische Wetenschappen, K.U. Leuven, Van Evenstraat 4, B-3000 Leuven, Belgium
E-mail: peter.dewitte@pharm.kuleuven.be

Key words: aggregation, photosensitizer, photodynamic therapy, hypericin, tumors, macrophages, monocytes

Introduction

Hypericin, a polycyclic aromatic naphthodianthrone constituent (Fig. 1) of the plant genus Hypericum, is a potent photosensitizer for photodynamic therapy (PDT) of tumors. Hypericin has proven to selectively accumulate in tumor tissue and to induce a pronounced antitumoral effect upon light irradiation (1,2). After intraperitoneal administration of 5 mg/kg hypericin, a 16-fold higher concentration of hypericin in tumor tissue versus surrounding healthy tissue was found in a subcutaneous P388 lymphoma tumor (3). Similar encouraging results were found with RIF-1 fibrosarcoma tumors (4). Moreover, a study performed with radioactive ^{123}I-labeled hypericin showed that the selective tumor accumulation is not dependent on the amount administered, as the maximal retention of radioactivity in tumor tissue was similar for the carrier-added and no-carrier added conditions (5).

Hypericin, which is almost insoluble in water, disperses in a physiological aqueous environment, producing non-fluorescent high molecular weight aggregates (6). Stability studies previously performed in our laboratory demonstrated that both the formulation of hypericin concentrates and the storage temperature have a substantial impact on the formation of aggregates. It was shown that polar organic solvents (e.g., polyethylene glycol) form stable fluorescent solutions, whereas aqueous vehicles were associated with a loss in photoactive content during storage and only partially released their hypericin content when applied to cells (7). Of importance, hypericin aggregates can also be formed during synthetic work, i.e. when the time of irradiation necessary to convert proto-hypericin via an oxidative photocyclization reaction into hypericin, is inadequately long.

Despite the fact that in the presence of lipoproteins blood-borne hypericin aggregates can readily dissociate into the monomeric form (8,9), we noticed in the course of a preliminary study that i.v. administration of aggregated compound strongly hindered a selective accumulation in tumor tissue. In this work we examined quantitatively the impact of aggregates present in the delivery mixture on the biodistribution of hypericin. For that purpose, we compared the *in vivo* tissue accumulation after administering hypericin suspended as coarse aggregates in phosphate-buffered saline, with the biodistribution found after injection of a solution of hypericin in a mixture of DMSO, polyethylene glycol and water. To support

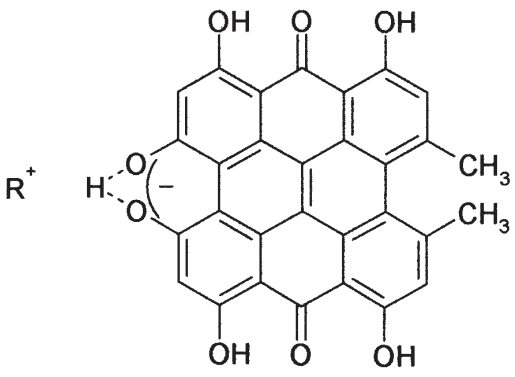

Figure 1. Chemical structure of hypericin present as a monobasic anion in physiological conditions.

our quantitative results histologically and to further explore the impact of the mononuclear phagocytic system on the tissue accumulation of aggregates, we examined several tissues by fluorescence microscopy, and studied the uptake of the aggregates by tissue macrophages.

Materials and methods

Synthesis of hypericin. Hypericin was synthesized from emodin anthraquinone according to Falk *et al* (6). Briefly, emodin (2.5 g), isolated from cortex Frangulae, was dissolved in 125 ml acetic acid and a solution of 5.0 g $SnCl_2.2H_2O$ in 65 ml concentrated hydrochloric acid was added. The mixture was refluxed for 3 h at 120˚C and emodin anthrone was precipitated by cooling to room temperature. To prepare protohypericin via oxidative dimerization, 2.0 g emodin anthrone was dissolved in 44 ml pyridine/piperidine (10/1) and 4 mg of pyridine-1-oxide and 100 mg of $FeSO_4.7H_2O$ were added. The reaction mixture was heated at 100˚C for 1 h under nitrogen in the dark. Protohypericin was precipitated in hexane and purified with silica column chromatography (mobile phase: ethylacetate/water with increasing amounts of acetone). A Sephadex LH-20 column (Pharmacia, Uppsala, Sweden) was used for further purification with dichloromethane, acetone and methanol as eluents. The compound was irradiated in acetone with a halogen lamp to undergo an oxidative photocyclization reaction to hypericin ($\varepsilon_{EtOH,\ 592}$: 45000 M^{-1} cm^{-1}). All manipulations with the photosensitizer were performed under strictly subdued light conditions (<1 μW/cm^2).

Animals and tumor system. The mouse RIF-1 (radiation-induced fibrosarcoma) tumor model was used. Cells ($1x10^6$) (kindly provided by Dr F. Stewart, The Netherlands Cancer Institute, Amsterdam, The Netherlands) were inoculated subcutaneously (s.c.) on the depilated lower dorsum of female C_{3H}/Km mice [weight range 21-25 g, purchased from Charles River Laboratories (France) or B&K Grimston (England)]. Tumors were grown to a surface diameter of about 3 mm and to a thickness of 1.5 mm, as measured by a calliper. Tumors grew in the s.c. space and were firmly attached to the overlying skin but generally not to the underlying musculature. All aspects of the animal experiment and husbandry were carried out in compliance with national and European regulations and were approved by the Animal Care and Use Committee of K.U. Leuven.

Hypericin whole body distribution. Hypericin was injected i.v. via a tail vein of mice at a dose of 20 mg/kg, either as a solution (i.e., dissolved hypericin) or as a suspension of coarse aggregates (i.e., aggregated hypericin). To prepare the solution, hypericin was firstly dissolved (8 mg/ml) in a mixture of dimethyl sulfoxide (DMSO) and polyethylene glycol (PEG) 400 (50/50), immediately before injection followed by adding an equal volume of water. A suspension of coarse aggregates was prepared by diluting instantly a concentrated solution of hypericin in DMSO (50 mg/ml) with PBS down to a final concentration of 4 mg/ml. The suspension was then sterilized in a capped glass vial by autoclaving (15 min at 121˚C). Tumor-bearing animals were sacrificed at several time-points after injection of hypericin. Tissue samples (skin, muscle, tumor, liver, spleen and lung) were harvested, weighed and frozen at -20˚C until determination of hypericin content. Consequently, the minced tissue was homogenized in tetrahydrofuran (THF) (Applichem Darmstadt, Germany) using a tissue homogenizer. Blood samples were mixed with THF immediately after harvesting and centrifuged (5 min at 14000 rpm). THF was chosen as an extraction solvent on the basis that it readily dissolves large hypericin aggregates forming fluorescent monomers. The supernatants were evaporated to dryness under reduced pressure followed by redissolving the residues in 0.25 ml DMSO (Acros Organics, NJ, USA) and fluorescence determination using a Microplate Fluorescence Reader (FL 600, Bio-Tek Instruments, Winooski, VT, USA) with excitation and emission filters of 530 and 645 nm, respectively. Similar tissue samples were also taken from control mice receiving no drug. Hypericin concentrations were calculated from a calibration curve subtracting background fluorescence present in control samples, as previously described (4). Graphical analysis was performed using Prism 4.00, GraphPad Software, San Diego, CA, USA.

Microscopic examination. Localization of hypericin was studied in tumors and in different organs rich in reticuloendothelial tissue 24 h after i.v. administration of hypericin. After sacrifice of the animals, tissue samples were immediately mounted in medium (Tissue Tek embedding medium, Miles, Elkhart, IN, USA) and immersed in liquid nitrogen. Different serial cryostat sections (5 μm slices) were taken from each sample. The first of three serial sections was examined by fluorescence microscopy (Axioskop 2 plus fluorescence microscope, Carl Zeiss, Göttingen, Germany), the second and third were immunologically stained with respectively BM8, a monoclonal antibody against the F4/80 antigen present on murine tissue macrophages, or MOMA-2, a monoclonal antibody for the broad detection of monocytes and macrophages in mice (Acris Antibodies, Hiddenhausen, Germany). To visualize specifically hypericin, Zeiss filter set 14 (BP 510-560 nm, LP 590 nm) was used. Fluorescence images were acquired using a light-sensitive charge-coupled device digital camera (AxioCam HR, Carl Zeiss). A KS imaging software system (Carl Zeiss, Vision, Hallbergmoos, Germany) was used.

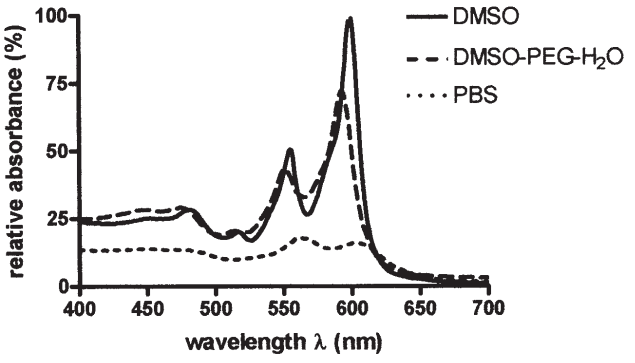

Figure 2. Absorption spectra of hypericin (20 μM) in DMSO, DMSO-PEG400-H_2O (25:25:50, V/V) and in PBS.

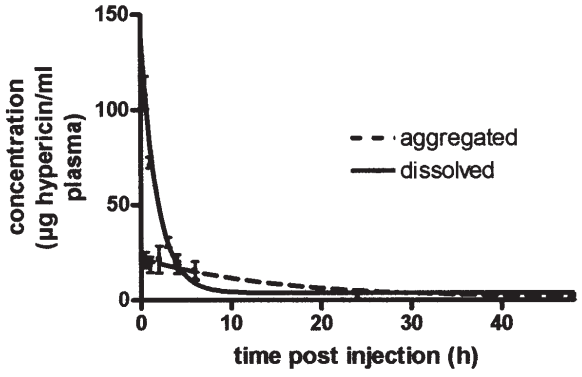

Figure 4. Plasma concentration of hypericin, expressed as μg/ml plasma, as a function of the time after i.v. injection of dissolved (in DMSO-PEG-H_2O) or aggregated (in PBS) hypericin.

Results

After preparation, the DMSO-PEG-H_2O solution looked clear without any visible particles and exhibited intense fluorescence upon UV irradiation. The absorbance spectrum was very similar to the one found for hypericin in pure DMSO, in which the compound is completely soluble (Fig. 2). On the contrary, the spectral shape of hypericin dispersed in PBS was markedly affected, with a strong reduction in absorbance and fluorescence yield, due to the aggregated condition of hypericin. Microscopic examination revealed that the size of coarse particles ranged from 5 to 30 μm.

The biodistribution of hypericin after i.v. injection of a solution or coarse aggregates is presented in Fig. 3. Hypericin accumulation (expressed in μg/g tissue) was determined for skin, muscle, tumor, liver, spleen and lung at 6, 24, 48 and 72 h after injection. After injection of dissolved hypericin, a gradual decrease in tissue concentration as a function of time could be seen for all tissues. Maximal uptake was at 6 h, with concentrations ranging from 1.9 μg/g in muscle to a maximum of 54 μg/g in lung tissue. Highly vascularised tissues, such as liver, spleen and lung showed a rapid decrease in hypericin content. For instance, concentrations at 24 h dropped to 9.8, <5 and 24%, respectively as compared to the peak levels measured at 6 h. Tumor levels decreased more slowly from 9.5 μg/g at 6 h to 4.9 μg/g at 24 h. In contrast, after injecting coarse aggregates, hypericin concentrations on the whole remained stable during the first 72 h after injection. Most interestingly, in this case values of about 300 μg/g were reached in spleen tissue. Also liver and lung tissue were hardly cleared from aggregates with high concentrations remaining at 48 and 72 h. Plasma values of aggregated hypericin at 0.5 h were only 20% of the amount after injection of dissolved hypericin (Fig. 4). Table I shows hypericin accumulation ratios of the coarse

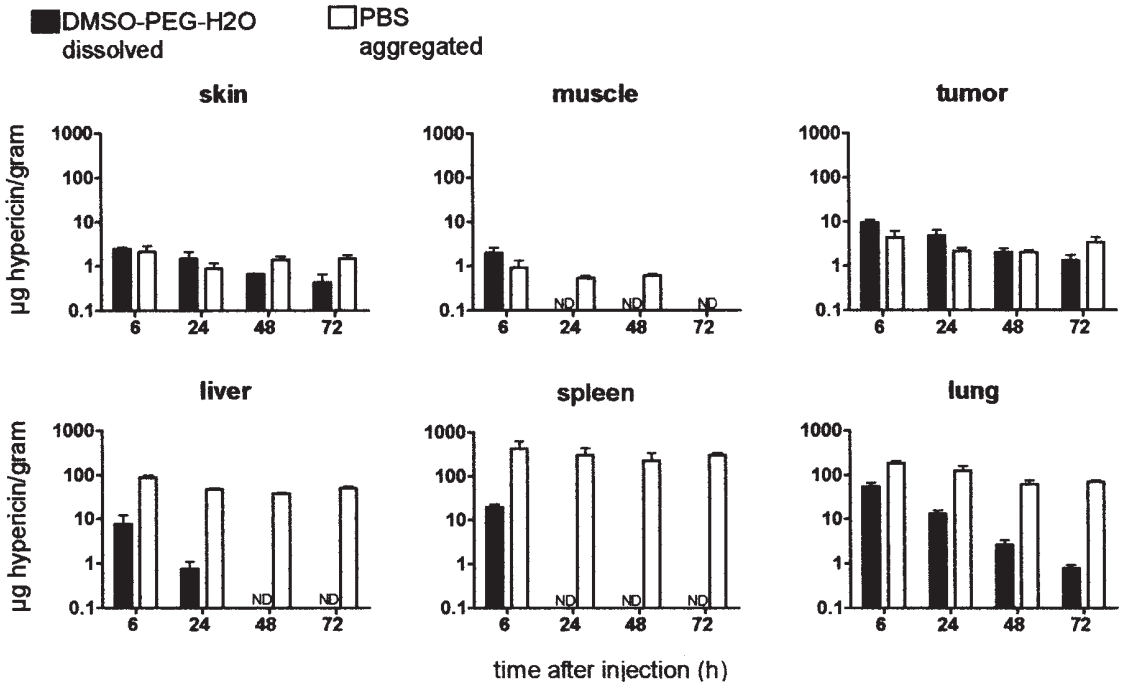

Figure 3. Hypericin accumulation (expressed in μg/gram tissue) after i.v. injection (20 mg/kg) of dissolved or aggregated hypericin. ND, not detectable.

Table I. Comparison between average tissue hypericin concentrations after injection of aggregated hypericin or dissolved hypericin ($[hypericin]_{aggregated}/[hypericin]_{dissolved}$).

	6 h	24 h	48 h	72 h
Liver	11.4	62.1	>50	>65
Spleen	22.3	>302	>228	>303
Lung	3.4	9.6	23.4	88.6

aggregates to dissolved hypericin. Ratios were very high in liver, spleen and lung, reaching values of >65, >303 and 89 respectively, at 72 h. Consequently, tumor/normal tissue ratios were extremely low for these three organs after injection of the coarse aggregates (Table IIA). We obtained ratios far less than 1 for liver, spleen and lung, which remained low during the whole experiment. At 24 h liver and lung exhibited respectively a 22- and 33-fold higher accumulation of hypericin as compared to tumor, while concentrations in spleen reached values which were 142 times higher than the ones found in tumor tissue. On the contrary, after injection of dissolved hypericin (Table IIB) significantly higher tumor/normal tissue ratios were found.

To elucidate the exact localization of hypericin in both conditions, a fluorescence microscopy study was performed on sections of spleen, liver, lung and tumor tissue. At 24 h after injection, fluorescence in liver tissue was faint and homogeneous for dissolved hypericin (Fig. 5A), whereas bright fluorescent spots covering the entire liver section could be found in case coarse aggregates were injected (Fig. 5B). These findings were confirmed for spleen and lung tissue. Detailed microphotographs and corresponding staining revealed the presence of fine particles within the fluorescent spots. Particle size was in the range of 15 μm diameter in lung tissue and 2.5 μm diameter in liver and spleen. Particles were respectively located in the lung capillaries, liver sinusoids and in the splenic cord, without any indication of internalization in cells. No correlation could be found between the tissue distribution of the fluorescent spots and the anti-macrophage markers MOMA-2 (Fig. 5C) and BM8 (Fig. 5D). Tumors obtained from mice, injected with aggregated hypericin, were practically not fluorescent, except for occasional solitary fluorescent spots found in the tumor rim (data not shown).

Discussion

Upon formulation in aqueous polar media lipophilic photosensitizers tend to aggregate and precipitate, a considerable problem when preparing these compounds for parental administration (10). Besides, aggregated photosensitizers have no use in PDT as they show a dramatic decrease in intersystem crossing quantum yields as compared to the corresponding solutions, with consequent lack of photochemical activity. Also in case of hypericin, oligomers are formed in an aqueous environment as a result of its hydrophobic aromatic core and hydrophilic perimeter (9,11).

We found evidence that extensive aggregation of hypericin, when prepared in PBS, strongly hinders an effective tumor targeting. The fast clearance of aggregates from plasma within 0.5 h is in line with a pronounced uptake of coarse aggregates in liver, spleen and lung, organs rich in reticuloendothelial tissue. Obviously, hydrophobic interactions between individual hypericin molecules, typically caused by a salting-out environment like PBS, triggered the formation of large aggregates that could no longer be monomerized efficiently by lipoproteins after i.v. injection. Presumably, the injection concentrate in PBS contained a mixture of coarse aggregates, colloidal hypericin and a small amount of monomeric hypericin. In contrast, hypericin delivered in a mixture

Table II. Comparison of average tumor/non-tumor uptake ratios ± standard deviation after i.v. injection (20 mg/kg) of A, aggregated; or B, dissolved hypericin.

A, Aggregated	6 h	24 h	48 h	72 h
Tumor/skin	2.780±1.600	4.040±2.600	1.140±0.400	2.670±1.000
Tumor/muscle	6.400±4.500	4.920±1.600	2.860±0.800	>7.100
Tumor/liver	0.046±0.036	0.044±0.014	0.053±0.012	0.061±0.035
Tumor/spleen	0.010±0.008	0.007±0.002	0.008±0.003	0.011±0.006
Tumor/lung	0.024±0.019	0.030±0.038	0.045±0.031	0.050±0.032

B, Dissolved	6 h	24 h	48 h	72 h
Tumor/skin	3.710±0.500	3.400±0.500	3.030±0.700	3.290±1.200
Tumor/muscle	5.130±1.400	>13.100	>2.770	>2.610
Tumor/liver	1.680±1.200	7.370±4.500	>2.640	>1.700
Tumor/spleen	0.610±0.400	>6.540	>2.010	>1.300
Tumor/lung	0.180±0.100	0.310±0.200	0.790±0.100	1.620±0.400

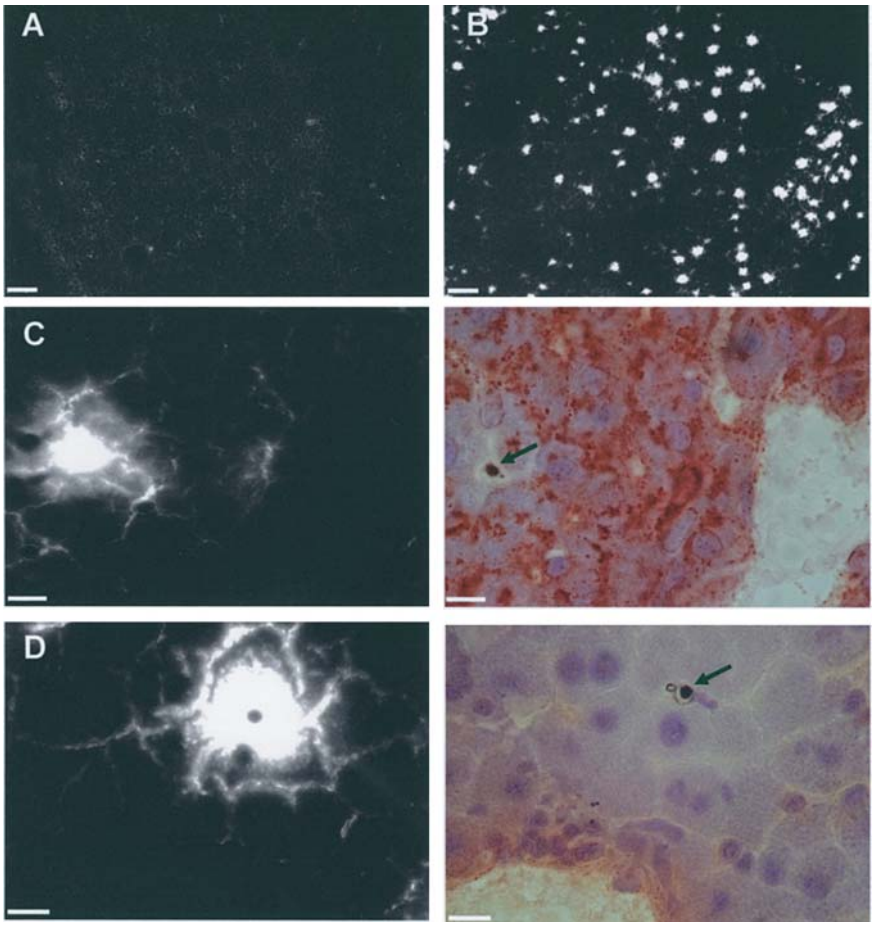

Figure 5. Fluorescence photomicrographs of 5 μm sections of liver tissue obtained from animals injected with dissolved hypericin (A) and aggregated hypericin (B). (C and D), detailed fluorescence photomicrographs of liver and corresponding staining with respectively MOMA-2 and BM8. Arrows mark particles present in the fluorescent centre. Scale bar (A and B), 100 μm. Scale bar (C and D), 10 μm.

of DMSO, PEG400 and water, resulted in favourable tumor to normal tissue ratios and a relatively fast elimination from the body. These data corroborate previously reported results using different formulations of photosensitizers (12,13). Thus, the nature of the vehicle was found to be of critical importance to the tissue distribution of hypericin, as it determines the physicochemical interactions of the compound and the transfer to lipoproteins, both before and after injection.

To reveal a possible role of the phagocytic system in the elimination of hypericin aggregates from the blood and to study the influence of macrophages and monocytes in tissue accumulation, we performed an additional fluorescence microscopy study. In tissues taken from mice injected with aggregated hypericin, a spot-like distribution of fluorescence could be observed with one or more particles in each fluorescent centre. As aggregates do not fluoresce, we believe that these bright spots were due to a local process of monomerization of hypericin. However, a phagocytic intervention of the mononuclear system could not be found as there was no correlation between the fluorescent pattern and BM8 or MOMA-2 stained monocytes and macrophages. The lack of a phagocytic intervention might be due to the large particle size as it has been demonstrated that liver macophages, Kupffer cells, only phagocyte small colloids of <0.1 μm (14). Likely, within 0.5 h p.i., the majority of aggregates are extracted by the pulmonary arterial bed on the first pass through the lung. Because the smallest lung capillaries have an internal diameter of approximately 8 μm, large aggregates will obstruct the alveolar capillary segments by physical entrapment (14). Blood cell bombardment and movement within arterioles may then cause particle fragmentation, followed by fast passage through the lungs and localization in liver and spleen, where they in turn become entrapped within the liver sinusoids and splenic cord (14). Physical entrapment of aggregates in lung, liver and spleen is confirmed by our quantitative results, where a slow elimination from liver, spleen and lung is obtained. In contrast, hypericin delivered as a solution, is fast and efficiently cleared from these organs. We also found that the presence of aggregates lowers the hypericin content in tumor tissue during the first 24 h. This is not surprising when taking into account the large amounts of hypericin that are consumed by entrapment in liver, spleen and lungs.

We could not detect any particles of hypericin in the DMSO-PEG-H_2O concentrate by means of microscopic examination. However, we cannot rule out that non-visible particles (<0.1 μm) were present. It can be assumed that if potential micro-particles do not become completely dissolved in the bloodstream by delivering their content to lipoproteins and albumin, a certain amount of hypericin will follow the pathway as described for the coarse aggregates, thereby

reducing the tumoritropic characteristics of the compound. Conversely, if this situation could be prevented, a further enhancement of the tumor/non-tumor tissue ratios of hypericin can be expected. However, the use of other parental formulations based on Cremophor-EL and polyvinyl pyrrolidone (PVP) in which hypericin was completely dissolved before i.v. injection, did not result in any further improvement of the tumoritropic character of the compound (data not shown). Likely, from a certain particle size on, hypericin monomers are readily released in their bio-environment for which they display a high affinity.

In conclusion, our results show that it is of critical importance to release hypericin in the bloodstream in a dissolved or colloidal form. Therefore, the delivery vehicle should prevent extensive aggregation before injection assuring an efficient transfer to serum lipoproteins upon injection. We demonstrated that coarse aggregates, formed in a PBS based delivery vehicle, result in an aspecific tissue accumulation of hypericin. Aggregates get trapped within tissues of the reticuloendothelial system, followed by a gradual monomerization. A direct involvement of monocytes and macrophages could not be demonstrated. These results may also be extended to radiolabeled derivatives of hypericin and other lipophilic photosensitizers, such as porphyrins, phthalocy-anines, naphthalocyanines and chlorins, with similar aggregation properties.

Acknowledgements

The authors thank Paula Aertsen and Gerda Luyckx (Department of Pathology) for excellent technical assistance. This study was supported by grants awarded by Fonds voor Wetenschappelijk Onderzoek-Vlaanderen (FWO Vlaanderen) and a Geconcerteerde Onderzoeksactie (GOA) of the Flemish Government.

References

1. Chen B, Zupko I and De Witte PA: Photodynamic therapy with hypericin in a mouse P388 tumor model: vascular effects determine the efficacy. Int J Oncol 18: 737-742, 2001.
2. Chen B, Roskams T and De Witte PA: Antivascular tumor eradication by hypericin-mediated photodynamic therapy. Photochem Photobiol 76: 509-513, 2002.
3. Chen B and De Witte PA: Photodynamic therapy efficacy and tissue distribution of hypericin in a mouse P388 lymphoma tumor model. Cancer Lett 150: 111-117, 2000.
4. Chen B, Xu Y, Roskams T, Delaey E, Agostinis P, Vandenheede JR and De Witte P: Efficacy of antitumoral photodynamic therapy with hypericin: relationship between biodistribution and photodynamic effects in the RIF-1 mouse tumor model. Int J Cancer 93: 275-282, 2001.
5. Bormans G, Huyghe D, Christiaen A, *et al*: Preparation, analysis and biodistribution in mice of iodine-123 labelled derivatives of hypericin. J Labelled Compd Radiopharm 47: 191-198, 2003.
6. Falk H, Meyer J and Oberreiter M: A convenient semisynthetic route to hypericin. Monatsh Chem 124: 339-341, 1993.
7. Huygens A, Kamuhabwa AR and De Witte PA: Stability of different formulations and ion pairs of hypericin. Eur J Pharm Biopharm 59: 461-468, 2005.
8. Lavie G, Mazur Y, Lavie D and Meruelo D: The chemical and biological properties of hypericin - a compound with a broad spectrum of biological activities. Med Res Rev 15: 111-119, 1995.
9. Falk H and Meyer J: On the homo- and heteroassociation of hypericin. Monatsh Chem 125: 753-762, 1994.
10. Konan YN, Gurny R and Allemann E: State of the art in the delivery of photosensitizers for photodynamic therapy. J Photochem Photobiol B 66: 89-106, 2002.
11. Yamazaki T, Ohta N, Yamazaki I and Song PS: Excited-state properties of hypericin: electronic spectra and fluorescence decay kinetics. J Phys Chem 97: 7870-7875, 1993.
12. Jori G, Reddi E, Cozzani I and Tomio L: Controlled targeting of different subcellular sites by porphyrin in tumour-bearing mice. Br J Cancer 53: 615-621, 1986.
13. Richter AM, Waterfield E, Jain AK, Canaan AJ, Allison BA and Levy JG: Liposomal delivery of a photosensitizer benzoporphyrin derivative monoacid ring A (BPD), to tumor tissue in a mouse tumor model. Photochem Photobiol 57: 1000-1006, 1993.
14. Kowalsky RJ and Falen SW: Radiopharmaceuticals. In: Nuclear Pharmacy and Nuclear Medicine. Landis NT (ed.) American Pharmacists Association, Washington, pp561-596, 2004.